

Computing the Magic Wavelengths for a Rubidium Atomic Lattice

A. Renn

L3 Computing Project, Group C2

Submitted: March 12, 2021

The optical lattice is a great tool for trapping atoms for atomic spectroscopy, however by trapping the atoms, it shifts their energy levels. We describe a computational technique for finding 'magic wavelengths' for a transition where both energy levels involved in the transition are shifted by the same energy, irrespective of the electric field strength. Rubidium-85 is used as our atom of interest and compute the magic wavelengths for the $5P_{1/2} \rightarrow 6S_{1/2}$ and $5P_{3/2} \rightarrow 6S_{1/2}$ transitions.

1. INTRODUCTION

Precise time and frequency measurement is an extremely important concept for modern physics and technology. Our best methods to get such a precise measurement are atomic clocks [1]. Using a laser to provoke electronic transitions in an atom proves to be an extremely precise method of timekeeping, provided a precise enough laser can be created [2]. One example of this is in Rubidium, where a clock transition could be from the $5P_{1/2}$ or $5P_{3/2}$ states to the $6S_{1/2}$ state [3]. These are shown in figure 1, as well as electric dipole transitions to and from these two states. To make a time measurement, this laser is tuned to the atomic transition frequency, for example by using the fluorescence of natural decay and a feedback loop which changes the laser frequency. Once the laser is on resonance with the transition frequency, the precise frequency of the laser is known and so this frequency can be counted to obtain a time measurement. Atomic clocks have many uses, for example: GPS (the Global Positioning System); to set the international time and frequency standard; and to control frequencies for fiber-optic internet communications.

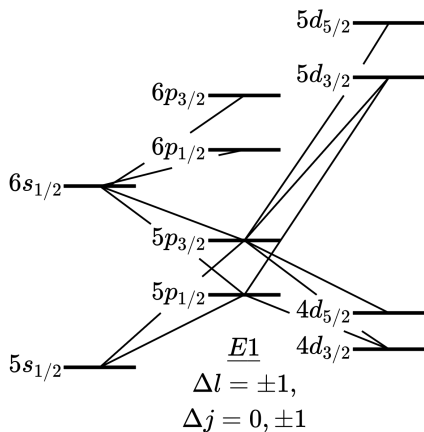


FIG. 1: A diagram of some of the energy levels of Rubidium with energies greater than its ground state ($5S$). Drawn also are all electric dipole transitions between these levels, and labelled are the selection rules for such a transition. For a more accurate and complete version of this, see figure 5.

To get the most precise atomic clocks however, the atoms which are probed must be extremely cold. This must be the case so that the atoms' movement is suppressed, so that they

can be probed by the laser for a long time to get a high averaging time. The low temperature also reduces the linewidth of the transition from Doppler broadening. The most common way to cool atoms is with laser cooling, which is very versatile, but can only cool atoms to a minimum Doppler temperature [4]. Another method - used in clocks such as the aluminium single-ion clock - is the Linear Paul Trap [5], but this trap only works for ions and has limitations on accuracy due to the Allan variance [3].

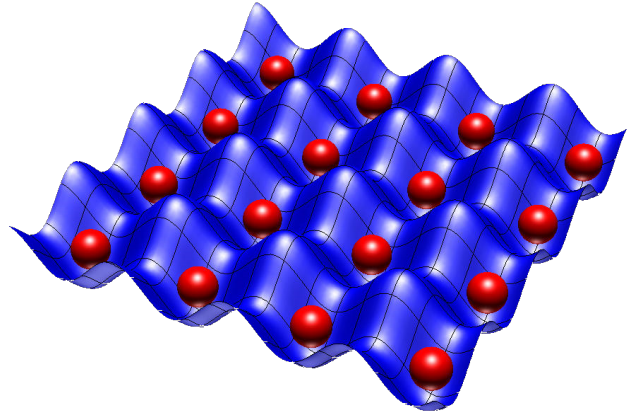


FIG. 2: A pictorial representation of a 2D optical lattice. The red spheres represent atoms and the blue background represents the potential of the trap. Credit: NIST, July 6 2009, ref 09PHY016.

This report will focus on a more novel technique - the optical lattice [6]. These work by having counter-propagating lasers in each cardinal direction which create standing waves of intensity, and via the dipole force [7], these intensity-standing waves correspond to potential standing waves. This is shown in figure 2 and means that if an atom is pre-cooled (e.g. by laser cooling) to lower than the maximum potential, it can be loaded into the optical lattice. It will then oscillate around the potential, and mostly there will only be one atom per well. Cooling can be aided by techniques such as Sisyphus cooling [4], and evaporation [8], which leaves fewer atoms in the trap, but most of the atoms are in their motional ground state. This is called the Lamb-Dick regime [9], and is when an optical clock has the highest precision.

Unfortunately, the dipole force which constrains the atoms to the trap also shifts the energy levels via the AC stark effect [7].

This AC stark effect gives an energy level shift ΔE , described by

$$\Delta E = -\frac{1}{2}(E)^2\alpha_J, \quad (1)$$

where E is the electric field strength, and α_J is the polarizability of the state with total angular momentum J (calculated with equations 3 and 4).

Since the energy shift depends on J , each of the energy levels is shifted by a different amount, which means that the clock frequency transition wavelength would be different for atoms in the optical lattice. This is a problem as this transition must be constant for an accurate measurement. However, there is a solution - 'magic' wavelengths can be found, at which the two levels of the clock transition have their energies shifted by the same amount, so that the transition frequency between them stays invariant.

The polarizability is a complex term, but a first-order perturbation theory derivation can be completed, as in [10]. This means that only electric dipole transitions are considered, which is appropriate as magnetic dipole and electric quadrupole transitions are a lot less probable, so contribute minimally to the polarizability. Finally, then, the polarizability is given by

$$\alpha_J = \alpha'_0(\omega) + \alpha''_2(\omega), \quad (2)$$

where $\alpha'_0(\omega)$ is the static polarizability of atomic state ν and $\alpha''_2(\omega)$ is the tensor polarizability of atomic state ν . Both of these depend on the frequency ω of the lattice lasers. Then, the static polarizability α'_0 is given by

$$\alpha'_0(\omega) = \frac{2}{3(2j_\nu + 1)} \sum_k \frac{\langle k||d||\nu \rangle^2 (E_k - E_\nu)}{(E_k - E_\nu)^2 - \omega^2}, \quad (3)$$

where j_k and j_ν are the total angular momenta of states k and ν , $\langle k||d||\nu \rangle$ is the reduced matrix element (RME) of the transition between states k and ν , and E_k and E_ν are the energies of states k and ν .

Then, the tensor polarizability is given by

$$\begin{aligned} \alpha''_2(\omega) = & -4C \sum_k (-1)^{j_\nu + j_k + 1} \begin{Bmatrix} j_\nu & 1 & j_k \\ 1 & j_\nu & 2 \end{Bmatrix} \\ & \times \frac{3m_j^2 - j_\nu(j_\nu + 1)}{j_\nu(2j_\nu - 1)} \times \frac{\langle k||d||\nu \rangle^2 (E_k - E_\nu)}{(E_k - E_\nu)^2 - \omega^2}, \\ C = & \left(\frac{5j_\nu(2j_\nu - 1)}{6(j_\nu + 1)(2j_\nu + 1)(2j_\nu + 3)} \right)^{\frac{1}{2}}, \end{aligned} \quad (4)$$

where j_k , j_ν , E_k , E_ν , and $\langle k||d||\nu \rangle$ have the same meanings as above, m_j is the total orbital quantum number corresponding to j_ν , and $\{\dots\}$ is the Wigner-6j symbol [11].

These expressions are complex, but the main takeaways from them are as follows:

- $(E_k - E_\nu)$ is equivalent to the transition frequency, meaning that when the laser frequency ω is tuned to this

value, the polarizability would reach infinity. This is unphysical, and corresponds to the fact that if the trapping laser wavelength was on-resonance with a transition frequency, all the atoms would be forced to transition into a different state, rather than be trapped by the laser.

- $\langle k||d||\nu \rangle$ represents the strength of a transition, and so is greater for more probabilistic transitions. This falls off as the quantum number n increases, meaning we only have to consider a finite number of states k for an accurate final polarizability.
- The remainder of equations 3 and 4 equate to constants, based on the quantum numbers of the state under consideration, so the polarizability is dependent on the two above points.

If we can compute this polarizability for a number of states, we can find points where it is the same value for our two transitions of interest: $5P_{1/2} \rightarrow 6S_{1/2}$; and $5P_{3/2} \rightarrow 6S_{1/2}$, which from this point will be coloured red, green, and blue for clarity.

2. METHODS

These calculations of polarizability require computational power. We use python to find the polarizability for many different wavelengths of light, and then numerical techniques are utilised to find the intersections of these curves.

As seen in equations 3 and 4, the energy and RME for each energy level considered is required. For this, we use ARC, an alkali atom calculator [12], which uses the method of quantum defects [12] to generate energies for each state. Then, for each of the energy levels considered ($5P_{1/2}$, $5P_{3/2}$, and $6S_{1/2}$), and for each wavelength in the range considered, all other energy levels up to $n = 15$ are summed over, using equations 3 and 4. Finally, we find the points where the curves cross, and use linear interpolation to find each magic wavelength. The gradient of each magic wavelength can also be found, which will be useful when deciding which wavelengths to use.

To complete the process, these magic wavelengths can be compared with the wavelengths of some commonly available lasers, but this is more useful when a practical implementation of the optical lattice is desired. This paper simply shows the feasibility of the techniques used.

3. RESULTS

Figures 3 and 4 show the polarizability of the discussed states over the range 550-650 nm. This range is picked as it is a common range for laboratory-grade lasers. The polarizability - and not the energy shift - is given because the energy shift differs based on the electric field, which differs based

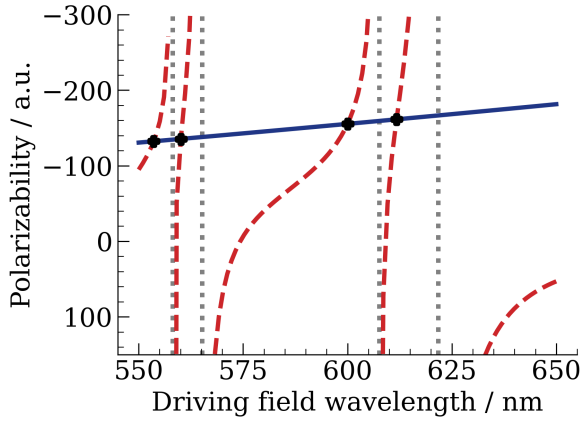


FIG. 3: The polarizability of the $5P_{1/2}$ (dashed red) and $6S_{1/2}$ (solid blue) states. Magic wavelengths are plotted as black points.

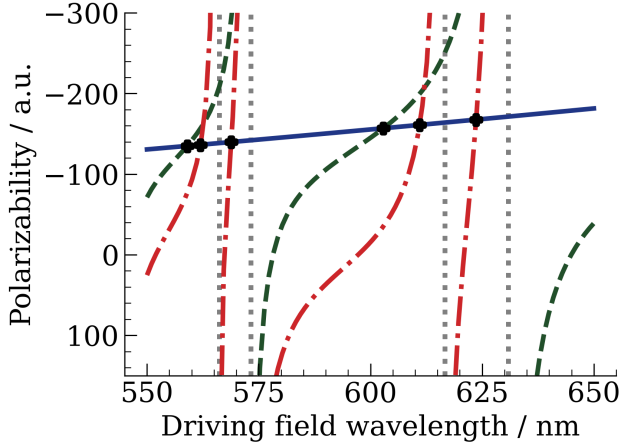


FIG. 4: The polarizability of the $5P_{3/2}[m_j = \pm 3/2]$ (dashed green), $5P_{3/2}[m_j = \pm 1/2]$ (dashed-dotted red), and $6S_{1/2}$ (solid blue) states. Magic wavelengths are plotted as black points.

on where the atom currently is in the optical lattice's potential well. Note that this polarizability is given in atomic units (a.u.) for ease of computation, and can be converted to SI ($\text{Hz m}^2 \text{V}^{-2}$) by multiplying by 2.48832×10^{-8} [10]. The vertical scale is also reversed, as negative polarizability corresponds to a positive energy shift, as in equation 1.

Figures 6 and 7 show the polarizability of the discussed states over another common laser wavelength range: 1200-1600 nm. All of these four figures have magic wavelengths shown in black, which are tabulated in table I.

Figure 5 is provided to help understand where the resonances in figures 3, 4, 6, 7 come from. The energy and transition wavelength of light is related by $E \propto \lambda^{-1}$. This means that a transition of 2 eV corresponds to a wavelength of 621 nm, and 1 eV to 1240 nm. Drawn on figure 5 are the 550-650 nm and 1200-1600 nm ranges, re-expressed as ranges of energy. It can be seen, then, that each dotted resonance on figures 3, 4, 6, 7

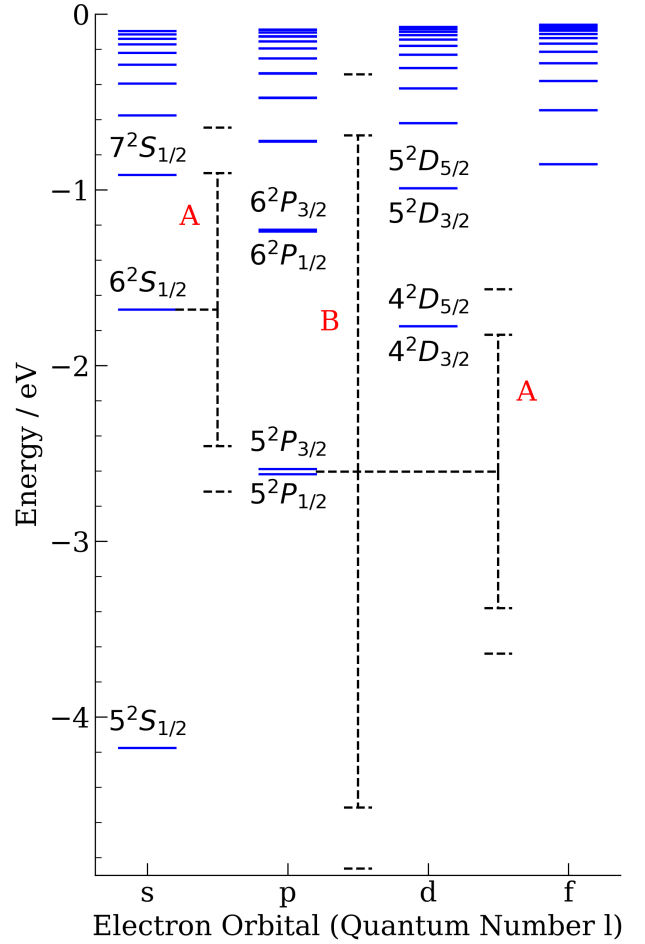


FIG. 5: A diagram of the energy levels used in the derivation. Some states are labelled, and they continue in this pattern up to $n = 15$. Also shown are the ranges of wavelengths used in the other figures in this paper. **A** shows the wavelength range 1200-1600 nm, and **B** shows the range 550-650 nm. Note that each resonance in figures 3, 4, 6, 7 can be linked to a transition in this graph, as shown in appendix B.

corresponds to the transition to an energy level in this range. This is shown in greater detail in appendix B.

Figure 8 shows the results of the computation with various different maximum energy levels considered. This illustrates the numerical convergence of the technique, as n increases, the graph changes less and less, and more accurate values of the magic wavelengths are converged upon. This is seen more clearly in appendix A. For the final results, a maximum n of $n = 15$ is used. This is good compromise between accuracy and computation time.

4. DISCUSSION

This investigation shows that magic wavelengths can be found for many transitions with relative ease. A lot of them, however, are unusable. This can be because of a few reasons,

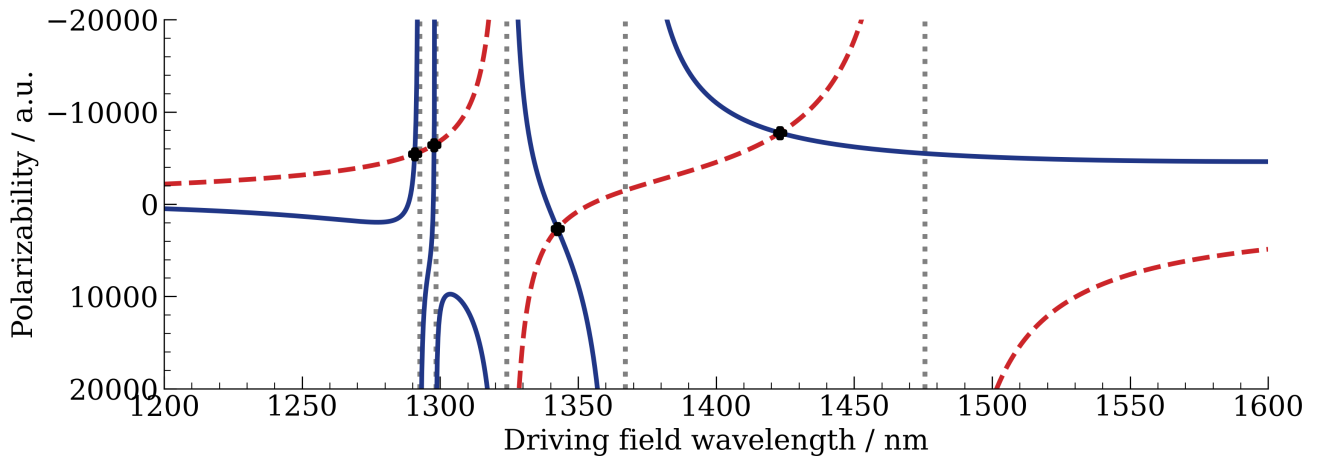


FIG. 6: The polarizability of the $5P_{1/2}$ (dashed red) and $6S_{1/2}$ (solid blue) states. Magic wavelengths are plotted as black points.

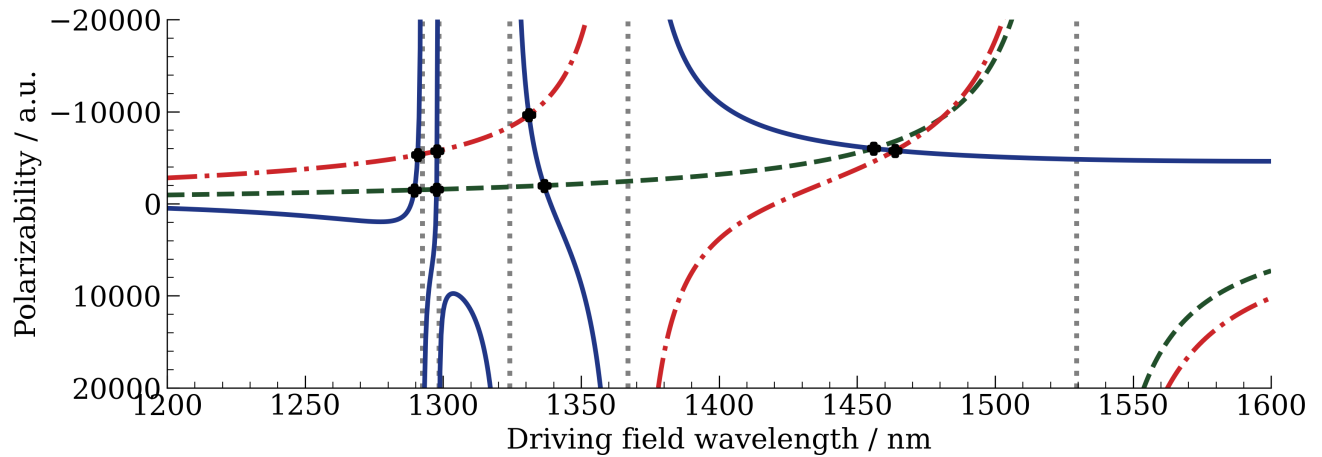


FIG. 7: The polarizability of the $5P_{3/2}[m_j = \pm 3/2]$ (dashed green), $5P_{3/2}[m_j = \pm 1/2]$ (dashed-dotted red), and $6S_{1/2}$ (solid blue) states. Magic wavelengths are plotted as black points.

and prompts the question 'What makes a good magic wavelength?'

One reason a magic wavelength can be of poor quality is because the gradient is far too steep, as with the values of 1290, 1291, and 1298 nm from table I. This is why these were not mentioned in [3]. This means that unless the setup were exactly tuned to the magic wavelength, a small electric field would incite a large energy shift and the energy levels would once again shift by a different amount, as is not desired. Therefore, in our final consideration, magic wavelengths with a very low gradient relative to the others are preferred.

Another reason a magic wavelength is considered unhelpful is if it is too close to the transition wavelength of interest. In this case, this is 1324 nm for the $5P_{1/2} \rightarrow 6S_{1/2}$ transition and 1367 nm for the $5P_{3/2} \rightarrow 6S_{1/2}$ transition (as shown in table I). This wavelength is in the second (lower energy) range which we consider. Therefore, the magic wavelengths of 1343, 1337, and 1331 nm might not be preferable for an experiment where the transition probability must be

carefully controlled. In this case, a magic wavelength in the 550-650 nm range may be preferable. Finally, from a practical point of view, a good magic wavelength is also one which is achievable by a modern laser system. For example, laser-diodes can easily achieve wavelengths of 554 or 560 nm.

An interesting question to consider is whether a 'triple' magic wavelength can be found. This would be a wavelength where three energy levels are shifted by the same amount. It would be near-impossible to find a perfect one, where all three curves cross at the same point, but given a large-enough precision, it is not unreasonable that one could find a wavelength where energy levels were energy-shifted by similar amounts. For example, just in this report, there is a magic wavelength at 600 nm for the $5P_{1/2} \rightarrow 6S_{1/2}$ transition and a magic wavelength at 603 nm for the $5P_{3/2}[m_j = \pm 3/2] \rightarrow 6S_{1/2}$ transition. These are also relatively low-gradient transitions, so a laser tuned to 601 nm may be able to keep the relative shift of these three levels quite similar. This is especially true if the final electric field value is low, as the error in the energy shift

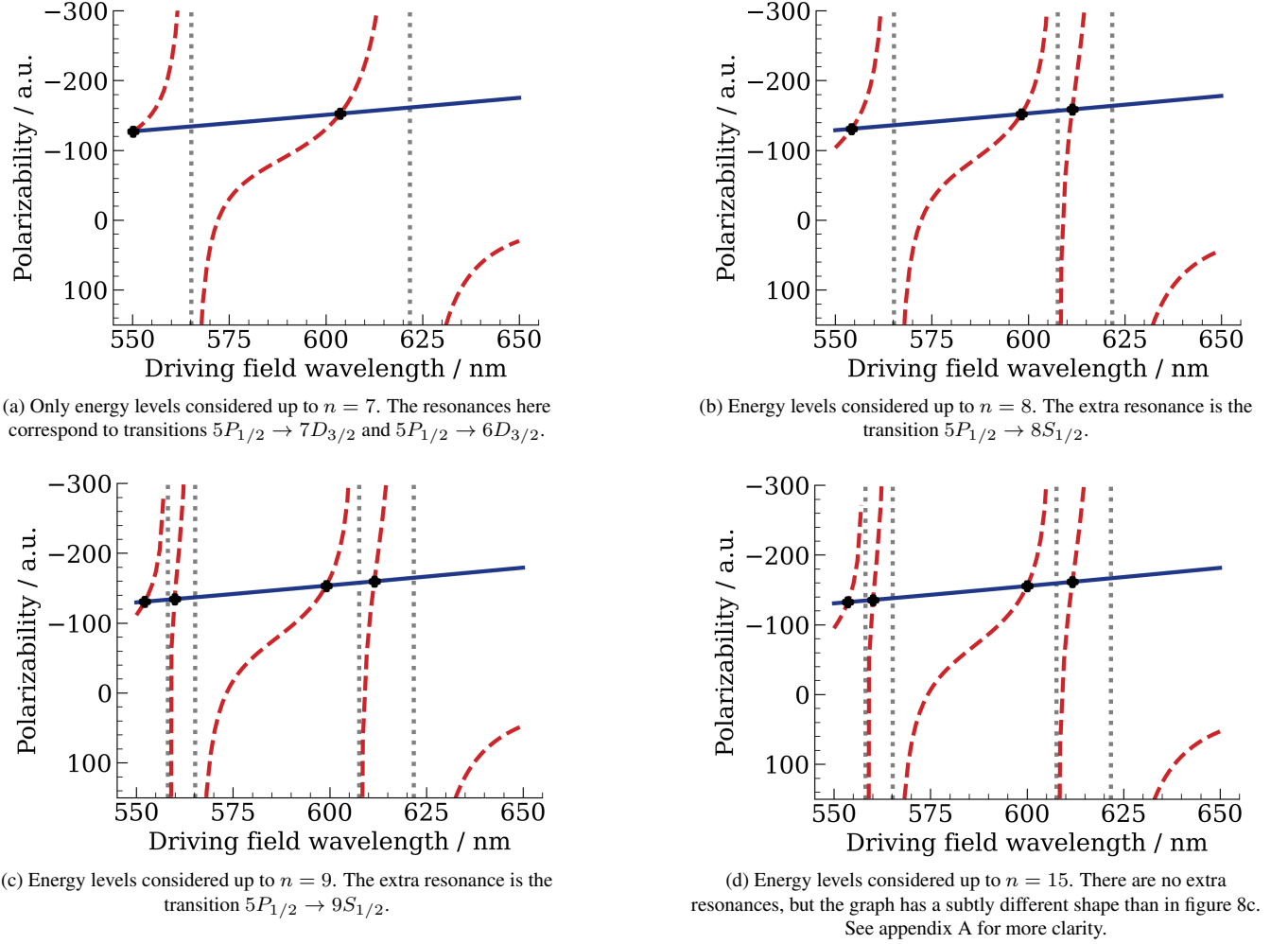


FIG. 8: A comparison of derivations with different maximum energy levels considered. Note, after the transitions exit the wavelength range considered, increasing N has less and less of an effect on the graph. This is illustrated via an animated gif in appendix A.

is proportional to $(E)^2$ (see equation 1), so if the atoms were in a motional ground state the optical lattice lasers could be reduced in intensity to the point at which they only just contain the atoms, and then experiments could be done involving all of the $5P_{1/2}$, $6S_{1/2}$, and $5P_{3/2}[m_j = \pm 3/2]$ transitions.

Next, the numerical convergence of the results is briefly discussed. As seen in figure 8, with each new energy level considered, the final output graph changes. Appendix A shows that each new energy level's contribution diminishes as you get to higher and higher n , but this alone is not enough to conclude that that is the case. Consider what happens as n is increased, in terms of what is seen in equations 3 and 4. As larger n is reached, the term $(E_k - E_\nu) - \omega^2$ increases, as the transition wavelength becomes further from the wavelength range considered. Then, one must know what happens to the $\langle k || d || \nu \rangle^2$ term. This is more nuanced, but it can be proved that this decreases for larger n , as transitions to larger n become less and less probable. Combining these two results,

it can be seen that as k (representing n) increases in the sum, the term inside the sum will diminish. This shows that as higher and higher n is considered, the contribution to the polarizability decreases. Therefore, we do not need to consider infinite energy levels, but only use up to a sensible number, like the $n = 15$ used in this report.

Finally, it is useful to consider avenues of further investigation, and techniques which may have helped this report. Firstly, the program could be further developed by computing energy levels of states from first principles, rather than using [12]. This would have the benefit of being more robust and being able to consider more different types of atoms, like group 2 atoms, but also the results might end up being further from reality, if for example instead the measured energy levels were used.

Next, there is a question of considering higher maximum energy levels. We stop at $n = 15$ in this report to strike a balance between accuracy and computation time, but if maximal accu-

Magic Wavelength / nm	Maximum gradient / a.u. nm ⁻¹	Literature wavelength / nm
$5P_{1/2} \rightarrow 6S_{1/2}$. Transition wavelength = 1324 nm		
554	-14.1	-
560	-84.3	-
600	-11.9	595
612	-41.0	612
1291	-5050	-
1343	717	1342
1423	-189	1421
$5P_{3/2}[m_j = \pm 3/2] \rightarrow 6S_{1/2}$. Transition wavelength = 1367 nm		
559	-6.38	-
603	-4.30	-
1290	-1680	-
1298	-11,100	-
1337	915	1336
1456	-89.0	1453
$5P_{3/2}[m_j = \pm 1/2] \rightarrow 6S_{1/2}$. Transition wavelength = 1367 nm		
562	-27.6	-
569	-87.4	-
611	-36.0	-
624	-67.3	-
1291	-5050	-
1298	-58,900	-
1331	2240	1331
1464	-165	1461

TABLE I: Each of the magic wavelengths from figures 3, 4, 6, 7. Also shown are the gradient of the steeper polarizability curve at this wavelength, for comparison. Each transition also has written the transition wavelength.

racy were required, a lot higher maximal energy levels could be considered. However, due to diminishing returns, this does become a fruitful activity at a certain point. As such $n = 15$ is deemed a suitable stopping point.

Finally, a branching path would be to look into hyperfine transitions. These types of transitions are more commonly used in atomic clocks, like the caesium clock, so could be more practically useful to know about. This would involve a slightly different derivation of equation 1, as the nuclear spin would have to be taken into account.

5. CONCLUSIONS

In conclusion, it is found that a first-order perturbation theory calculation in order to compute polarizabilities works well for finding magic wavelengths, and many can be found. The best of these are 600, 603, and 562 nm, which are far from the transition wavelength of interest, and also far from any transition resonances, to minimise the polarizability-gradient. This technique, however, only works very well for a single transition of interest, and works to an acceptable precision for two transitions. Further investigation could find magic wavelengths for different atoms, or work on improving the accuracy of the results computed here.

REFERENCES

- [1] T.L. Nicholson, S.L. Campbell, et al. *Systematic Evaluation of an Atomic Clock at 2×10^{-18} Total Uncertainty*. Nature Communications 6.1 (2015): 6896.
- [2] K. Hosaka, H. Inaba, et al. *Evaluation of an Ultra-stable Laser System Based on a Linewidth Transfer Method for Optical Clocks*. 2014 European Frequency and Time Forum (EFTF) (2014): 186-88.
- [3] X. Zang, Z. Tong-Gang, and J. Chen. *Magic Wavelengths for a Lattice Trapped Rubidium Four-Level Active Optical Clock*. Chinese Physics Letters 29.9 (2012): 4.
- [4] V. Ivanov, and S. Gupta. *Laser-driven Sisyphus Cooling in an Optical Dipole Trap*. ArXiv.org 84.6 (2011): ArXiv.org, Dec 23, 2011.
- [5] N. Herschbach, K. Pyka, et al. *Linear Paul Trap Design for an Optical Clock with Coulomb Crystals*. ArXiv.org 107.4 (2011): 891-906.
- [6] A. Derevianko, and H. Katori. *Colloquium: Physics of Optical Lattice Clocks*. ArXiv.org 83.2 (2010): 331-347.
- [7] *Laser Control of Atoms and Molecules*. Materials Today (Kidlington, England) 10.5 (2007): 57.
- [8] S. Kemp. *Laser Cooling and Optical Trapping of Ytterbium* (2017).
- [9] M. Mirzaee. *Quantum Dynamics of Ultra-cold Atoms in the Presence of Virtual Photons*. ArXiv.org (2017): ArXiv.org, May 27, 2017.
- [10] B. Arora, M. Safronova, and C. Clark. *Magic Wavelengths for the Np-ns Transitions in Alkali-metal Atoms*. ArXiv.org 76.5 (2007): 2.
- [11] A. Vincenzo, H. Haggard, et al. *Semiclassical Mechanics of the Wigner 6 J -symbol*. Journal of Physics A: Mathematical and Theoretical 45.6 (2012): 61.
- [12] N. Sibalic, J. Pritchard, C. Adams, and K. Weatherill. *ARC: An Open-source Library for Calculating Properties of Alkali Rydberg Atoms*. Computer Physics Communications 220.C (2017): 319-331.

Appendix A: Animated Gif

Figure 8 shows a few different values of maximum energy level n considered. For a gif of a range of n from $n = 5$ to $n = 20$ visit:

https://alifeee.co.uk/durham_physics/alt-max-n-gif.gif

Appendix B: Resonances

There are many resonances in figures 3, 4, 6, 7, corresponding to energy-level transitions in figure 5. They are listed in table II.

Transition	Wavelength / nm
Figure 3: $5P_{1/2} \rightarrow 6S_{1/2}$ from 550-650 nm.	
$5P_{1/2} \rightarrow 9S_{1/2}$	558.1
$5P_{1/2} \rightarrow 7D_{3/2}$	565.2
$5P_{1/2} \rightarrow 8S_{1/2}$	607.6
$5P_{1/2} \rightarrow 6D_{3/2}$	621.7
Figure 4: $5P_{3/2} \rightarrow 6S_{1/2}$ from 550-650 nm.	
$5P_{3/2} [m_j = \pm 1/2] \rightarrow 9S_{1/2}$	566.2
$5P_{3/2} \rightarrow 7D_{3/2}$	573.2
$5P_{3/2} [m_j = \pm 1/2] \rightarrow 8S_{1/2}$	616.7
$5P_{3/2} \rightarrow 6D_{3/2}$	630.8
Figure 6: $5P_{1/2} \rightarrow 6S_{1/2}$ from 1200-1600 nm.	
$6S_{1/2} \rightarrow 7P_{3/2}$	1292.5
$6S_{1/2} \rightarrow 7P_{1/2}$	1298.5
$6S_{1/2} \rightarrow 5P_{1/2}$	1324.1
$6S_{1/2} \rightarrow 5P_{3/2}$	1367.0
$5P_{1/2} \rightarrow 4D_{3/2}$	1475.9
Figure 7: $5P_{3/2} \rightarrow 6S_{1/2}$ from 1200-1600 nm.	
$6S_{1/2} \rightarrow 7P_{3/2}$	1292.5
$6S_{1/2} \rightarrow 7P_{1/2}$	1298.5
$6S_{1/2} \rightarrow 5P_{1/2}$	1324.1
$6S_{1/2} \rightarrow 5P_{3/2}$	1367.0
$5P_{3/2} \rightarrow 4D_{5/2}$	1529.5

TABLE II: Tabulated are the resonances (dotted grey lines) from figures 3, 4, 6, 7. These are listed in order of wavelength, so are ordered left-to-right on the graphs.